Journal Pre-proofs

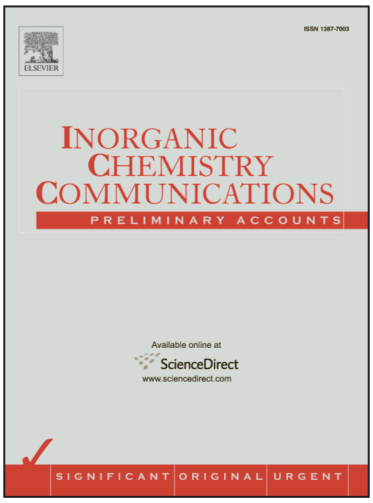

Short communication

An unprecedented binodal (4,6)-connected Co(II) MOF as dual-responsive luminescent sensor for detection of acetylacetone and Hg^{2+} ions

Yu-Qiao Su, Yun-Hua Qu, Lianshe Fu, Guang-Hua Cui

PII: S1387-7003(20)30603-1
DOI: https://doi.org/10.1016/j.inoche.2020.108013
Reference: INOCHE 108013

To appear in: *Inorganic Chemistry Communications*

Received Date: 19 April 2020
Revised Date: 3 June 2020
Accepted Date: 4 June 2020

Please cite this article as: Y-Q. Su, Y-H. Qu, L. Fu, G-H. Cui, An unprecedented binodal (4,6)-connected Co(II) MOF as dual-responsive luminescent sensor for detection of acetylacetone and Hg^{2+} ions, *Inorganic Chemistry Communications* (2020), doi: https://doi.org/10.1016/j.inoche.2020.108013

An unprecedented binodal (4,6)-connected Co(II) MOF as dual-responsive luminescent sensor for detection of acetylacetone and Hg^{2+} ions

Yu-Qiao Su[a], Yun-Hua Qu[a], Lianshe Fu[b], Guang-Hua Cui[a]*

[a]College of Chemical Engineering, Hebei Key Laboratory for Environment Photocatalytic and Electrocatalytic Materials, North China University of Science and Technology, No. 21 Bohai Road, Caofeidian new-city, Tangshan, Hebei, 063210, P. R. China

[b]Department of Physics and CICECO-Aveiro Institute of Materials, University of Aveiro, 3810-193 Aveiro, Portugal.

Corresponding author: Guang-Hua Cui

Fax: +86-315-8805462. Tel: +86-315-8805460.

E-mail: tscghua@126.com

Abstract

A new Co(II) organic framework, $\{[Co_2(L)(hfpd)(H_2O)]\cdot 1.75H_2O\}_n$ (**1**) (H_4hfpd = 4,4'-(hexafluoroisopropylidene)diphthalic acid, L = 4,4′-bis(imidazol-1-yl)-biphenyl) was hydrothermally synthesized and characterized. **1** possesses an unusual (4,6)-connected layered network architecture. Fluorescence titration results presented that **1** is rarely dual-responsive probe to detect acetylacetone and Hg^{2+} ions by luminescence quenching.

Keywords: Acetylacetone; Cobalt(II) MOFs; Crystal structure; Dual luminescent sensor; Hg^{2+} ions; Rigid ligand

Introduction

Mercury compounds are applied in electronics, chemical, pharmaceutical, biological and other aspects, which is frightening toxic to humans and the environment.[1,2] In the environment, ionic mercury is converted into neurotoxic methylmercury by bacteria. Even minor quantity of bioaccumulated mercury can cause health problems related to vital body organs like the spinal cord, kidney, etc.[3] Acetylacetone (acac) is generally performed as an intermediate in organic synthesis, an analytical reagent for extraction separation, a sol-gel modifying agent, and a chelating agent in sol–gel process.[4–6] Nevertheless, as a toxic chemical, acetylacetone causes severe harm to human health when ingested or inhaled, accompanied by signs of headaches, nausea, vomiting and dizziness.[7] The United States Environmental Protection Agency (US EPA) lists the limits and standards for the emission of acac and Hg^{2+} ions, which are classified as a group A carcinogen.[8,9] There are numbers of methods to recognize and quantify acac and mercury ions, but most of them are low effective and time-consuming and expensive.[10] Therefore, it is very important to develop suitable probes to detect acac and Hg^{2+} ions.[11,12]

As a multifunctional crystalline porous material, metal–organic frameworks (MOFs) have been explored in various applications like fluorescence sensitization, drug delivery, catalysis, separation and gas storage.[13,14] Notably, luminescent MOFs (LMOFs) have obtained rapid development in recent years due to their favorable operability, short response time, excellent performance, and low cost,[15] and have been employed to identify heavy metal ions and small organic molecules.[16–24] Thus, LMOFs may serve as an available tool for detecting of Hg^{2+} ions and acac simultaneously.

Herein, a unique 2D cobalt–organic framework, $\{[Co_2(L)(hfpd)(H_2O)]\cdot 1.75H_2O\}_n$ (**1**) (L = 4,4′-bis(imidazol-1-yl)-biphenyl, H_4hfpd = 4,4'-(hexafluoroisopropylidene)diphthalic acid) was

reported. Luminescence titration experiment results show that **1** can act as a chemosensor toward acac and Hg^{2+} ions.

Results and discussion

1 crystallizes in triclinic space group *P*$\bar{1}$. The asymmetric unit of **1** consists of two Co(II) centers, one $hfpd^{4-}$ ligand, one L ligand, one coordinated water molecule, and 1.75 free H_2O molecules (Fig. 1a). The six-coordinated Co1(II) center has a slightly distorted octahedral {$CoNO_5$} coordination geometry and is surrounded by N atom (N4B, symmetry code: B = -*x*, -*y*+1, -*z*) from one L ligand, four oxygen atoms from three different $hfpd^{4-}$ ligands (O1, O4, O6 and O9C; symmetry code: C = -*x*+1,-*y*+2,-*z*+1), and an oxygen atom from a coordinated water molecule (O1W). The Co1–O/N bond distance ranges from 2.030(3) to 2.160(3) Å. The Co2(II) center coordinates with three oxygen atoms from one nitrogen atoms from one L ligand (N1) and three different $hfpd^{4-}$ ligands (O3, O5D and O9C). The four-coordinated Co2(II) center displays a distorted trigonal-pyramidal {$CoNO_3$} coordination geometry (τ_4 = 0.86). The Co2–O/N bond lengths range from 1.980(3) to 2.004(4) Å. The coordination angles around Co1 and Co2 are in the regions of 85.34(1)–177.58(1)° and 98.42(1)–125.54(2)°, respectively, which are similar to those of the reported Co(II) MOFs.[25]

The $hfpd^{4-}$ ligands adopt a (κ^1-κ^0)-(κ^1-κ^1)-(κ^1-κ^1)-(κ^1-κ^0)-μ_6 coordinating mode, linking the neighboring Co(II) centers to form a 1D infinite $[Co_2(hfpd)]_n$ chain, with a Co···Co separations of 3.480(1)–7.811(1) Å (Fig. S1). The L ligands adopt (κ^1)-(κ^1)-μ_2 *trans*-conformation and its two imidazole rings are parallel to each other. Further, the 1D $[Co_2(hfpd)]_n$ chains are further extended by L ligands into a 2D framework (Fig. S2), which can be simplified as a scarce 4,6-connected 2D framework with the symbol of $\{4^{11}.6^4\}\{4^3.6^3\}_2$. To the best of our knowledge, this type of topology in (4,6)-connected 2D network found in the MOFs is the first example. (Fig. 1b).

(Insert Fig. 1)

Thermogravimetric curves indicate that the MOF possesses highly thermal stability. **1** remains stable up to 336 °C (Fig. S3). The pure phases of **1** were evaluated by X-ray powder diffraction and the results suggest the bulk samples are highly agreement with the simulated one from single crystals of **1** (Fig. S4).

The emission spectra of **1** and free L ligands are gained in solid state at room temperature (Fig. S5). When the excitation wavelength is 274 nm, the free ligand L renders the maximum emission peak at 407 nm, which can be attributed to $\pi^*\rightarrow\pi$ *or* $\pi^*\rightarrow n$ electron transitions within the ligand L. The emission peak of **1** is 356 nm (λ_{ex} = 294 nm), compared with the ligand L, the emission peak of **1** blue-shifted by 51 nm, which may be derived from intra-ligand or ligand-to-ligand charge-transfer transition. Time-dependent emission spectra of **1** were measured by dispersion of **1** powder in aqueous solution or ethanol solution (Fig. S6), and the results show that **1** owns good dispersion and stability in solutions and the test time has little effect on the emission intensities of **1**. In addition, PXRD patterns for **1** powder after time-varying experiments either in aqueous solution or in ethanol solution further confirms that the structure of **1** was kept after immersed in solutions (Fig. S7).

The fluorescence spectra of **1** in different solvents (methanol (MeOH), ethanol (EtOH), ethylene glycol (EG), n-butanol (NB), *N*,*N*-dimethyl acetamide (DMA), *n*-methyl pyrrolidone (NMP), dimethyl sulfoxide (DMSO), acetonitrile (MeCN), dichloromethane (DCM), xylene (XY) and acac) are shown in Fig. 2a. It was affected by the polarity of solvent and the physical interaction between solute and solvent, **1** fluorescence intensity increased or decreased to some extent, in particular, the fluorescence intensity in acac was almost completely quenched. The quenching efficiency ($Q = (1 - I/I_0) \times 100\%$, Q is the quenching efficiency, I_0 and I are the luminescence

intensities without adding and adding acac) reaches 99.46% for **1**. Anti-interference experiments recorded **1** (4 mg) luminous intensity of the presence of acac (2 mL) and other organisms (2 mL) (Fig. S8) in which there is no significant difference, so **1** is immensely selective chemical sensor for detection of acac.

The acac titration experiment results show that the fluorescence intensity of **1**@acac suspension gradually decreases with the increase of acac concentration (Fig. 2b). Fluorescence enhancement can be attributed to solvent-induced energy transfer theory that rich electronic π-conjugated structure will help to increase the electron density of compound, enhance luminescence emission intensity.[26] The quenching behavior of acac of **1** can be fitted by the exponential quenching equation $I_0/I - 1 = \mathrm{Aexp(R[M])} + \mathrm{b}$ (A, R and b represent constants and [M] is the concentration of acac). The quenching behavior can be fitted to $I_0/I - 1 = 40.27 \times \exp(48.71 \times [\mathrm{M}]) - 40.38$ (Fig. S9). When the acac is at a low concentration, the linear relationship between concentration and quenching efficiency can be fitted using the Stern-Volmer (SV) formula: $(I_0/I) = 1 + K_{sv}[\mathrm{M}]$ (K_{sv} represents quenching constant). The value of K_{sv} can be calculated to be 1915 M^{-1}. The detection limit (LOD) of **1** for acac is 14 μM which calculated according to the formula: $\mathrm{LOD} = 3\sigma/k$ (σ is the standard deviation, and k is the slope of the quenching curve). Compared with the previously reported CP-based fluorescence probes for acac, **1** demonstrates unsatisfactory sensitivity in acac monitoring (Table S3).[27–30]

(Insert Fig. 2)

In view of the remarkable fluorescence emission of **1**, fluorescence sensing of various common cations was examined. As **1** had good fluorescence performance in EtOH solution, ethanol was finally selected as the dispersant of the reaction system. The experiment results show that the

common cations (Na^+, K^+, Mg^{2+}, Sr^{2+}, Ba^{2+}, La^{3+}, Sm^{3+}, Eu^{3+}, Tb^{3+}, Fe^{3+}, Co^{2+}, Ni^{2+}, Cu^{2+}, Ag^+, Zn^{2+}, Cd^{2+} and Hg^{2+}) exhibit varieties effects on the luminescence intensity of **1** (Fig. 3a). **1** exhibits the most noticeable turn-off luminescent quenching effect with Hg^{2+}. The anti-interference results show when Hg^{2+} ions coexist with other metal ions, fluorescence of suspension **1** is not be interfered (Fig. S10).

As shown in Fig. 3b, the fluorescence intensity of **1**@Hg^{2+}suspension gradually decreases with the increase of Hg^{2+} ions concentration, and the fluorescence is almost completely quenched when the concentration reaches 500 μM. The quenching behaviors of Hg^{2+} ions of **1** can be fitted by the exponential quenching equation $I_0/I-1 = A\exp(R[M]) + b$, [M] is the concentration of Hg^{2+} ions). The quenching behaviors can be fitted to $I_0/I-1 = 1.28 \times 10^{-2} \times \exp(1.5 \times 10^4 \times [M]) + 0.82$. As depicted in the inset in Fig. S11, there is a linear relationship when the Hg^{2+} ions are at low concentration range of 0–200 μM ($R^2 = 0.9851$). According to the Stern-Volmer equation, $I_0/I = 1 + K_{SV}[M]$, The quenching efficiency is proportional to Hg^{2+} ions concentration. The calculated value of K_{SV} is 6497 M^{-1}. The calculated value of LOD for Hg^{2+} ions is 4 μM, which is comparable to some other reported Hg^{2+} fluorescent sensing complexes, which indicates that **1** shows high sensitivity to detect Hg^{2+} ions (Table S4).[31–33]

(Insert Fig.3)

The possible fluorescence quenching mechanism of acac and Hg^{2+} ions toward **1** was analyzed. The PXRD results show that the diffraction patterns of **1** which soaked in acac/Hg^{2+} solutions are consistent with the initial ones, proving that fluorescence quenching is not caused by the decomposition of framework of **1** (Fig. S12). Besides, **1** shows excellent recyclable behaviors and can be recycled at least three times for sensing of acac and Hg^{2+} (Fig. S13). The spectral overlap of

the analyte's absorption band and the excitation band of MOFs determines the probability of resonance energy transfer. The UV−Vis spectra of acac/Hg^{2+} solutions were checked (Fig. S14). The absorption bands of acac (250−330 nm) and Hg^{2+} ions (200−280 nm) have a large overlap with the excitation bands of **1** (280−357 nm), indicating that the quenching process may be caused by the resonance energy transfer from the excited MOF **1** to the acac or Hg^{2+} ions.[34]

Conclusion

In summary, **1** was successfully synthesized and characterized under hydrothermal process. **1** depicts an unusual 2D network. The low detection limits (14 μM for acac and 4 μM for Hg^{2+}, respectively) and high quenching constant (1915 M^{-1} for acac and 6497 M^{-1} for Hg^{2+} respectively) suggest that **1** is a promising candidate as dual-functional luminescence sensor for detection of acac and Hg^{2+} ions.

Supplementary Material

CCDC 1958997 contains the supplementary crystallographic data for **1**. The data can be obtained free of charge *via* http://www.ccdc.cam.ac.uk/conts/retrieving.html, or from the Cambridge Crystallographic Data Centre, 12 Union Road, Cambridge CB2 1EZ, UK; fax: (+44) 1223-336-033; or e-mail: deposit@ccdc.cam.ac.uk.

Acknowledgments

The project was supported by the National Natural Science Foundation of China (51474086). This work was also developed within the scope of the project CICECO-Aveiro Institute of Materials, UIDB/50011/2020 & UIDP/50011/2020, financed by national funds through the Foundation for Science and Technology/MCTES.

References

[1] N. Issaro, C. Abi-Ghanem, A. Bermond. Anal. Chim. Acta 631 (2009) 1–12.

[2] G.F. Nordberg, B.A. Fowler, M. Nordberg. Handbook on the Toxicology of Metals. Academic press, 2014.

[3] I. Onyido, A.R. Norris, E. Buncel. Chem. Rev. 104 (2004) 5911–5930.

[4] M.M. Doroodmand, M.G. Kharekani, Chem. Eng. J. 283 (2016) 453–461.

[5] X. Wang, S. Wu, Z. Li, X. Yang, J. Hu, Q. Huo, J. Guan, Q. Kan, Appl. Organomet. Chem. 29 (2015) 698–706.

[6] M. Yu, M. Liang, J. Liu, S. Li, B. Xue, H. Zhao, Appl. Surf. Sci. 363 (2016) 229–239.

[7] X.M. Kang, R.R. Cheng, H. Xu, W.M. Wang, B Zhao. Chem. Eur. J. 23 (2017) 13289–13293.

[8] L. Zhou, C. Li, X. Weng. Magn. Reson. Chem. 54 (2016) 222–226.

[9] N. Bloom, W.F. Fitzgerald. Anal. Chim. Acta 208 (1988) 151–161.

[10] US Department of Health and Human Services, Toxicological profile for chromium, public health service agency for toxic substances and diseases registry, Washington, DC, 2005.

[11] K. Zheng, Z. Liu, Y. Jiang, P. Guo, H. Li, C. Zeng, S. Zhong. Dalton Trans. 47 (2018) 17432–17440.

[12] K. Zheng, Z. Q. Liu, Y. Huang, F. Chen, C. H. Zeng, S. Zhong, S.W. Ng. Sens. Actuators, B 257 (2018) 705–713.

[13] B.W. Qin, X.Y. Zhang, J.P. Zhang. Dyes Pigm. 174 (2020) 108011.

[14] L.L. Qian, Z.X. Wang, J.G. Ding, H.X. Tian, K. Li, B.L. Li, H.Y. Li. Dyes Pigm. 175

(2020) 108159.

[15] X.S. Zeng, H.L. Xu, Y.C. Xu, X.Q. Li, Z.Y. Nie, S.Z. Gao, D.R. Xiao. Inorg. Chem. Front. 5 (2018) 1622–1632.

[16] X.X. Wu, H.R. Fu, M.L. Han, Z. Zhou, L.F. Ma, Cryst. Growth Des. 17 (2017) 6041−6048.

[17] Z. Zhou, M.L. Han, H.R. Fu, L.F. Ma, F. Luo, D.S Li. Dalton Trans. 47 (2018) 5359–5365.

[18] Y.Q. Zhang, V.A. Blatov, T.R. Zheng, C.H. Yang, L.L. Qian, K. Li, B.L. Li, B Wu. Dalton Trans. 47 (2018) 6189–6198.

[19] P.F. Shi, H.C. Hu, Z.Y. Zhang, G. Xiong, B. Zhao. Chem. Commun. 51 (2015) 3985–3988.

[20] X.M. Kang, H.S. Hu, Z.L. Wu, J.Q. Wang, P. Cheng, J. Li, B. Zhao. Angew. Chem. Int. Ed. 131(2019) 16763–16769.

[21] X.L. Jiang, S.L. Hou, Z.H. Jiao, B. Zhao. Anal. Chem. 91 (2019) 9754–9759.

[22] N. Abdollahi, A. Morsali. Anal. Chim. Acta 1064 (2019) 119–125.

[23] Y.M. Zhu, C.H. Zeng, T.S. Chu, H.M. Wang, Y.Y. Yang, Y.X. Tong, W.T. Wong. J. Mater. Chem. A 1 (2013) 11312–11319.

[24] M.Q. Yang, C.P. Zhou, Y. Chen, J.J. Li, C.H. Zeng, S. Zhong. Sens. Actuators, B. 248 (2017) 589–596.

[25] Q.Q. Xiao, G.Y. Dong, Y.H. Li, G.H. Cui, Inorg. Chem. 58 (2019) 15696–15699.

[26] C. Liu, Liu, X. Liu, H. Chen, Z. Niu, H. Hirao, P. Braunstein, J. Lang. J. Am. Chem. Soc. 142 (2020) 6690–6697.

[27] H. Zhu, C. Han, Y.H. Li, G.H. Cui. J. Solid State Chem. 282 (2020) 121132.

[28] H. Zhu, L. Fu, D. Liu, Y. H. Li, G.Y. Dong. J. Solid State Chem. 286 (2020), 121265.

[29] X.M. Kang, R.R. Cheng, H. Xu, W.M. Wang, B. Zhao, Chem. Eur. J. 23 (2017) 13289–13293.

[30] S.L. Yao, S.J. Liu, X.M. Tian, T.F. Zheng, C. Cao, C.Y. Niu, Y.Q. Chen, J.L. Chen, H. Huang, H.R. Wen, Inorg. Chem. 58 (2019) 3578–3581.

[31] Z.J. Wang, L.J. Han, X.J. Gao, H.G. Zheng, Inorg. Chem. 57 (2018) 5232–5239.

[32] S.A.A. Razavi, M.Y. Masoomi, A. Morsali, Inorg. Chem. 56 (2017) 9646–9652.

[33] W.C. Kang, C. Han, D. Liu, G.H. Cui, Inorg. Chem. Commun. 106 (2019) 81–85.

[34] Y.Q. Zhang, V.A. Blatov, T.R. Zheng, C.H. Yang, L.L. Qian, K. Li, B.L. Li, B. Wu, Dalton Trans. 47 (2018) 6189–6198.

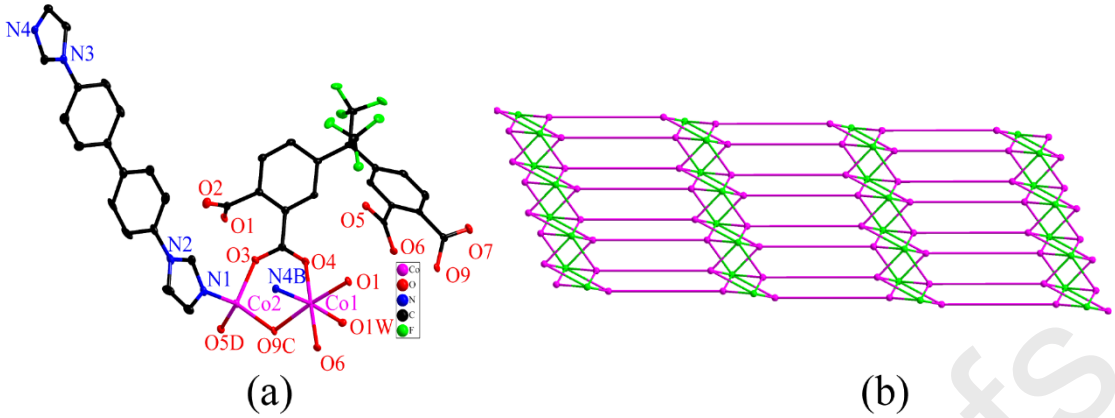

Fig. 1. (a) Coordination environment of Hg^{2+} ions in **1** with atom labelling scheme and thermal ellipsoids at 30% probability level. Symmetry codes for 1: A = *x*+1, *y*, *z*; B = -*x*, -*y*+1, –*z*; C = -*x*+1, -*y*+2,-*z*+1; D = -*x*, –*y*+2, –*z*+1; E = *x*-1, *y*, *z*; **(b)** The (4,6)-connected topological network of **1**.

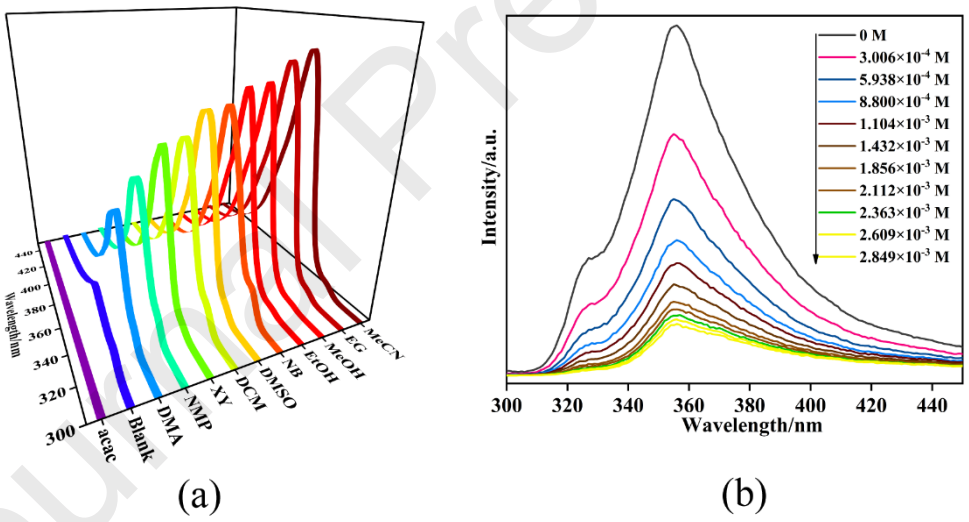

Fig. 2. (a) Luminescent intensities for **1** dispersed in aqueous solution upon the dropping of different organics; **(b)** Emission spectra of **1** dispersed in aqueous solutions with different concentrations of acac at room temperature.

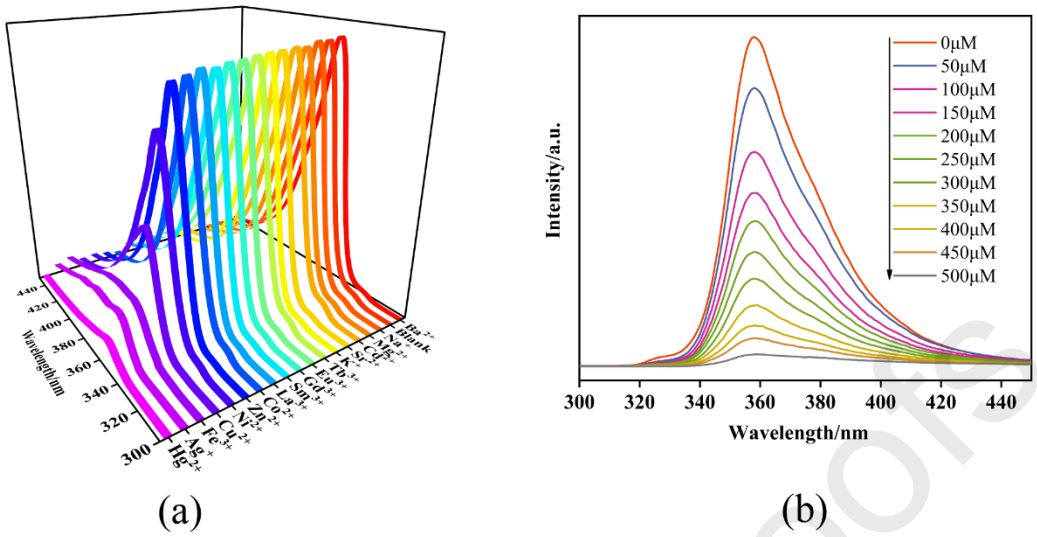

Fig. 3. (a) Luminescent intensities for **1** immersed in EtOH with various metal ions; **(b)** Emission spectra of **1** in EtOH suspension with different concentrations of Hg^{2+} ions.

Research highlights

►An unprecedented binodal (4,6)-connected Co(II) MOF was synthesized.

►Thermal stability and luminescence properties of **1** were investigated.

►**1** is rarely dual-responsive probe to detect acac and Hg^{2+} ions.

An unprecedented binodal (4,6)-connected Co(II) MOF as dual-responsive luminescent sensor for detection acetylacetone and Hg^{2+} ions

Yu-Qiao Su, Yun-Hua Qu, Lianshe Fu, Guang-Hua Cui

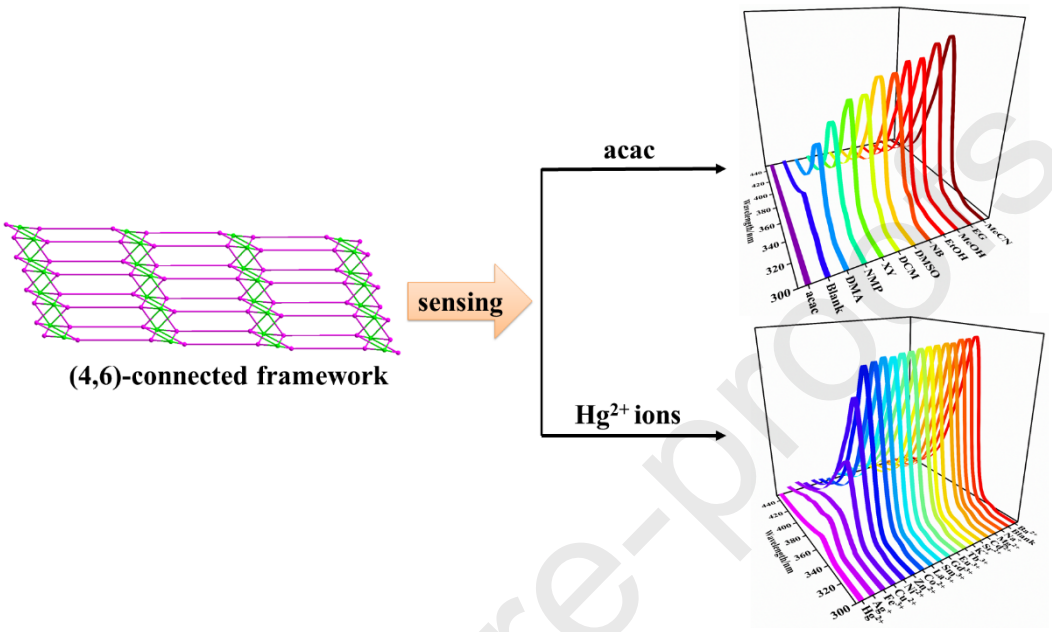

A new Co(II) organic framework, $\{[Co_2(L)(hfpd)(H_2O)]\cdot 1.75H_2O\}_n$ (**1**) was hydrothermally synthesized and characterized. **1** is a promising dual-functional sensor for detection of acac and Hg^{2+} ions by luminescence quenching.

Yu-Qiao Su: Methodology, Formal analysis, Investigation, Writing-Original Draft. **Yun-Hua Qu:** Software, Visualization, Data Curation. **Lianshe Fu:** Writing-Review & Editing, Data check and Validation. **Guang-Hua Cui:** Conceptualization, Writing Editing, Supervision, Project administration, Funding acquisition.